12-6-2022

Comparative study of differentiating human pluripotent stem cells into vascular smooth muscle cells in hydrogel-based culture methods

Qing Liu

Zhen Liu

Hongyu Gu

Yuxia Ge

Xuesheng Wu

See next page for additional authors

Authors

Qing Liu, Zhen Liu, Hongyu Gu, Yuxia Ge, Xuesheng Wu, Fuxing Zuo, Qian Du, Yuguo Lei, Zhanqi Wang, and Haishuang Lin

Regenerative Therapy 22 (2023) 39–49

Contents lists available at ScienceDirect

Regenerative Therapy

journal homepage: http://www.elsevier.com/locate/reth

Original Article

Comparative study of differentiating human pluripotent stem cells into vascular smooth muscle cells in hydrogel-based culture methods

Qing Liu [a, 1], Zhen Liu [b, 1], Hongyu Gu [c, 1], Yuxia Ge [d, 1], Xuesheng Wu [e, 1], Fuxing Zuo [f, 1], Qian Du [g], Yuguo Lei [h, ***], Zhanqi Wang [i, **], Haishuang Lin [d, *]

[a] Department of Obstetrics, Beijing Obstetrics and Gynecology Hospital, Capital Medical University, Beijing Maternal and Child Health Care Hospital, Beijing, 100006, China
[b] Department of Neurosurgery, Beijing Shunyi District Hospital, Beijing, 101300, China
[c] Department of Thoracic Surgery Ward 3, The First Hospital of Qiqihar, Affiliated Qiqihar Hospital, Southern Medical University, Qiqihar, 161005, China
[d] Department of Neurology, The Second Hospital of Harbin, Harbin, 150056, China
[e] Department of Chemical Biology, School of Pharmaceutical Sciences, Peking University, Beijing 100191, China
[f] Department of Neurosurgery, National Cancer Center/National Clinical Research Center for Cancer/Cancer Hospital, Chinese Academy of Medical Sciences and Peking Union Medical College, Beijing, 100021, China
[g] Department of Biological Systems Engineering, University of Nebraska-Lincoln, Lincoln, NE, 68588, USA
[h] Department of Biomedical Engineering, Huck Life Science Institute, Pennsylvania State University, University Park, PA, 16802, USA
[i] Department of Vascular Surgery, Beijing Anzhen Hospital of Capital Medical University, Beijing Institute of Heart Lung and Blood Vessel Diseases, Beijing, 100029, China

ARTICLE INFO

Article history:
Received 23 September 2022
Received in revised form
31 October 2022
Accepted 6 December 2022

Keywords:
Human pluripotent stem cells
PNIPAAm-PEG hydrogel
Alginate hydrogel fiber
Vascular smooth muscle cells
Industrial production

ABSTRACT

Vascular smooth muscle cells (VSMCs), which provides structural integrity and regulates the diameter of vasculature, are of great potential for modeling vascular-associated diseases and tissue engineering. Here, we presented a detailed comparison of differentiating human pluripotent stem cells (hPSCs) into VSMCs (hPSCs-VSMCs) in four different culture methods, including 2-dimensional (2D) culture, 3-dimensional (3D) PNIPAAm-PEG hydrogel culture, 3-dimensional (3D) alginate hydrogel culture, and transferring 3-dimensional alginate hydrogel culture to 2-dimensional (2D) culture. Both hydrogel-based culture methods could mimic *in vivo* microenvironment to protect cells from shear force, and avoid cells agglomeration, resulting in the extremely high culture efficiency (e.g., high viability, high purity and high yield) compared with 2D culture. We demonstrated hPSC-VSMCs produced from hydrogel-based culture methods had better contractile phenotypes and the potential of vasculature formation. The transcriptome analysis showed the hPSC-VSMCs derived from hydrogel-based culture methods displayed more upregulated genes in vasculature development, angiogenesis and blood vessel development, extracellular matrix compared with 2D culture. Taken together, hPSC-VSMCs produced from hydrogel-based culture system could be applied in various biomedical fields, and further indicated the suitable development of alginate hydrogel for industrial production by taking all aspects into consideration.

1. Introduction

Vascular smooth muscle cells (VSMCs) are one of the major cell types of blood vessel, and they play a critical role in the development, function and maintenance of vasculature [1,2]. VSMCs hold the great potential of vascular-associated disease modeling and drug discovery [3–6], tissue engineering [7–9] and cytotherapy [10,11]. However, a big challenge for those application mentioned above is how to get enough VSMCs from *in vitro* differentiation or primary tissues [1,12,13]. Currently, human pluripotent stem cells

* Corresponding author.
** Corresponding author.
*** Corresponding author.
E-mail addresses: yxl6034@psu.edu (Y. Lei), aresbill@outlook.com (Z. Wang), hlin9@bjmu.edu.cn (H. Lin).
Peer review under responsibility of the Japanese Society for Regenerative Medicine.
[1] These authors contributed equally to this work.

https://doi.org/10.1016/j.reth.2022.12.001

(hPSCs), possessing the ability of unlimited proliferate *in vitro* and differentiating into all somatic cell types of human body [14,15], could be used to resolve the obstacle. Especially, induced pluripotent stem cells (iPSCs) derived from patient cells or tissues retaining the patient's genetic information is suitable for modeling human diseases [16,17]. Recently, many protocols for effectively differentiating hPSCs into VSMCs have been developed, either through embryoid bodies [3,18,19] or monolayer culture [20,21]. The researchers are able to drive hPSCs differentiation into different regions of VSMCs [6,21–26]. For example, an efficient and simple protocol of VSMCs differentiation from hPSCs reported by Patsch has been established in 2D monolayer level in 6 days for a range of biological applications [20].

Although using the current protocols, producing large number of hPSC-VSMCs for various biological applications remains difficult. The traditional 2D monolayer cell culture generally produces a low cell yield [27,28]. The traditional 3D suspension culturing often form big agglomerates, which cause spontaneous differentiation in the central region of agglomerates, and limit cell proliferation [27], which are not suitable for large scale production. To resolve the limitations, we previously reported a high culture efficiency method for hPSCs expansion and differentiation [29–32]. Here, we represented and compared four different culture methods for hPSC derived VSMCs. Firstly, hPSCs are cultured in 3D PEG hydrogel and 3D alginate hydrogel, then they are differentiated into VSMCs. Secondly, we compared hPSC-VSMCs in different culture methods, including cell yield, differentiation efficiency, functional properties and the whole transcriptome gene expression. The results revealed that hPSC-VSMCs could be highly produced in the hydrogels-based culture methods, and hPSC-VSMCs produced from hydrogel-based culture methods had better contractile phenotypes and the potential of vasculature formation. The transcriptomic analysis showed the hydrogel-based culture methods displayed more upregulated genes in vasculature development, angiogenesis and blood vessel development, extracellular matrix compared with 2D culture. Taken all aspects into together, the alginate hydrogel-based culture methods will be suitable for the applications of hPSC-VSMCs in biological fields and industrial production.

2. Materials and methods

2.1. Cell culture

H9 hESCs (#WA09, WiCell) were purchased from WiCell Research Institute. H9 hESCs were maintained in 6-well plate coated with Matrigel in Essential 8™ medium. Cells were passaged every 4 days with 0.5 mM EDTA. Medium was changed daily. Cells were routinely checked for the expression of pluripotency markers, OCT4 and NANOG, and bacterial or mycoplasma contamination. HUVECs (#00191027, Lonza) were obtained from Lonza, and maintained in 10-cm dish with EGM™-2 Endothelial Cell Growth Medium-2 BulletKit™ (CC-3162). HUVECs were passaged every 3–4 days with 0.25% Trypsin–EDTA solution. Medium was changed daily.

2.2. Culturing hPSCs in 3D PNIPAAm-PEG hydrogels and alginate hydrogel fibers

The method for hPSCs culture in 3D PNIPAAm-PEG Hydrogels and alginate hydrogel fibers have been described in our previous publication [15,30,33]. The optimal concentration (10%) of PNlPAAm-PEG [15] and (1.5%) sodium alginate hydrogel [30] for hPSC biology and culture were determined in our previous studies. For 3D PNIPAAm-PEG Hydrogels culture, hPSCs were first dissociated into single cells, then mixed with 10% PNIPAAm-PEG solution dissolved in E8 medium on ice and cast on tissue culture plates, then incubated at 37 °C for 10 min to form hydrogels before adding warm E8 medium containing 10 mM ROCK inhibitor (LC Laboratories, no. Y5301). The medium was changed daily. Cells were passaged every 5 days. To quantify cells, the medium was removed, and 2 mL ice cold PBS was added to dissolve the hydrogel for 5 min. Cell spheroids were collected by spinning at 100 g for 3 min. Cells were dissociated into single cells in Accutase at 37 °C for 10 min, and counted cell with the TC20 automated cell counter and passage cells for the following culture.

For alginate hydrogel fibers culture, a hyaluronic acid (HA) or methylcellulose (MC) solution containing single cells and an alginate solution was pumped into the central and side channel of the home-made micro-extruder, respectively, and extruded into a $CaCl_2$ buffer (100 mM) to make hydrogel fibers. Subsequently, the $CaCl_2$ buffer was replaced by cell culture medium. For a typical cell culture, 20 μL of cell solution in hydrogel fibers were suspended in 2 mL E8 medium in a 6-well plate and cultured in an incubator. Medium was changed daily. To quantify cells, medium was removed and alginate hydrogels were dissolved with 0.5 mM EDTA for 5 min. Cell mass was collected by centrifuging at 100 g for 5 min, treated with Accutase at 37 °C for 12 min and dissociated into single cells, and counted cell with the TC20 automated cell counter and passage cells for the following culture.

2.3. Making hPSC-VSMCs in 2D culture, 3D PEG hydrogel or 3D alginate hydrogel fibers

Briefly, for VSMCs differentiation, hPSCs were first expanded according to different culture methods. Then, the medium was replaced with N2B27 medium (1:1 mixture of DMEM/F12 (#SH30004.04, HyClone) with Glutamax-I (#35050061, Life Technologies) and Neurobasal medium (#21103049, Life Technologies) supplemented with N2 (#17502048, Life Technologies) and B27 minus vitamin A (#12587010, Life Technologies) with 8 μM CHIR99021 (#C6556, LC laboratories) and 25 ng/mL BMP4 (#314BP010, R&D Systems). After 3 days, the medium was replaced by N2B27 medium supplemented with 10 ng/mL PDGF-BB (#100-14 B, PeproTech) and 2 ng/mL ActivinA (#338-AC, R&D Systems). The medium was exchanged every day. VSMCs were harvested for analysis on day 6 or day 10.

For transferring 3D alginate hydrogel culture to 2D culture, hPSC-VSMCs derived from alginate hydrogel were dissociated into single cell and replated into 2D culture for 6 days.

2.4. Immunocytochemistry

For 2D immunostaining, the 2D cells were fixed with 4% paraformaldehyde (PFA) at room temperature for 20 min, permeabilized with 0.25% Triton X-100 for 30 min, and blocked with 5% donkey serum for 1 h before incubating with primary antibodies: α-SMA (sc-130616, Santa Cruz), SM22A (ab14106, Abcam), Human-PDGFRB (PA5-14718, ThermoFisher), Human-CD31 (555444, BD Biosciences) at 4 °C overnight. After extensive washing, secondary antibodies (715-545-151, 711-585-152, 711-165-152, 705-605-147, Jackson ImmunoResearch) and 10 μM 4′, 6-Diamidino-2-Phenylindole (DAPI) in 2% BSA were added and incubated at room temperature for 4 h. Cells were washed with PBS for 3 times before imaging with A1 confocal microscope. For cell mass immunostaining, after fixation for 30 min, cell masses were incubated with PBS +0.25% Triton X-100 + 5% (vol/vol) goat serum + primary antibodies at 4 °C for 48 h. After extensive washing, secondary antibodies in 2% BSA were added and incubated at 4 °C for 24 h. Cells were washed with PBS three times before imaging with a confocal microscope. For 3D cell staining, VSMCs derived from 3D PEG-hydrogel and 3D-alginated hydrogel

were dissociated into single cells and replated into well-plate for 2 h, followed by fixed with 4% PFA, then performed the above immunostaining procedure.

2.5. Co-culture assay of HUVECs and hPSC-VSMCs

200 μL of Matrigel was added into each well of a 12-well plate and incubated for 30 min at 37 °C to allow the formation of a thin layer of hydrogel. For the functional tube formation and association assays *in vitro*, the HUVECs and the hPSC-VSMCs were prestained with DiI (red) and DiO (green), respectively, according to the manufacturer's instructions. Cells were grown in EGM-2 medium supplemented with 50 ng/mL VEGF-A. For the experiment, 2.0×10^4 HUVECs/cm^2 and 2.0×10^4 hPSC-VSMCs/cm^2 were co-cultured for 24 h in the incubator. Cells were fixed with 2% PFA for 10 min and analyzed using Zeiss fluorescence microscope.

2.6. Fibronectin production

After 5 days of differentiation, all VSMCs were seeded in N2B27 containing 10 ng/mL PDGF-BB at 40,000 cells/cm^2 on gelatin-coated wells. After 24 h, the medium was changed to N2B27 with 10 ng/mL PDGF-BB supplemented with DMSO or 2.5 ng/mL TGF-β. After 24 h, cells were washed with PBS, fixed with 4% PFA for 10 min at room temperature, and immunofluorescence staining of deposited Fibronectin (ab2413, Abcam) was performed.

2.7. Western blot analysis

After 5 days of differentiation, all VSMCs were seeded in N2B27 containing 10 ng/mL PDGF-BB at 40,000 cells/cm^2 on gelatin-coated wells. After 24 h, the medium was changed to N2B27 with 10 ng/mL PDGF-BB supplemented with DMSO or 2.5 ng/mL TGF-β. After 24 h, cells were washed with PBS, then were harvested and cell lysates were prepared using the Pierce IP™ lysis buffer (cat # 87788, ThermoFisher) supplemented with Halt™ Protease & Phosphatase Single-Use Inhibitor Cocktail (100x, cat # 78442, ThermoFisher). 30 μg of total proteins for each sample were subjected to SDS-PAGE analysis on a 4%–12% NuPAGE™ Bis-Tris protein gel (cat # NP0321BOX, ThermoFisher). GAPDH was used as a loading control. The membrane was blocked in TBST (Thermo Scientific) containing 5% nonfat dried milk (Applygen) and subsequently incubated with anti-Fibronectin antibody (1:3000, MA5-11981, ThermoFisher) at 4 °C overnight. The membrane was washed three times with TBST for 10 min and incubated with an anti-mouse/rabbit IgG secondary antibody conjugated to horseradish peroxidase (IgG-HRP; 1:3000; Santa Cruz) for 1 h at room temperature. Then, the membrane was washed three times with TBST for 10 min and imaged using a gel imaging system (Tanon).

2.8. Contraction study

VSMCs from 3D methods were first dissociated into single cells and replated into 2D plate. All VSMCs were seeded in N2B27 containing 2 ng/mL ActivinA and 2 μg/mL at 40,000 cells/cm^2 on Collagen-coated wells according to previous studies [20,34]. After 48 h, they were stained with 2.5 μM Fluo-4 AM (#50018, Biotium) at 37 °C for 1 h. Contraction was induced by treating the cells with 100 μM carbachol (#2810, Tocris). Contraction images of VSMCs were acquired by a Zeiss fluorescence microscope. The fluorescence intensity of intracellular calcium flux, cell surface area (mm^2) and percent change of cell surface area was assessed by choosing the same cell before and after drug treatment using ImageJ software.

2.9. Matrigel plug assay

Animal procedures were performed in accordance with an IACUC-approved protocol reviewed by the University of Nebraska–Lincoln Animal Care and Use Committee. 6–8 week old female SCID mice (Charles River Laboratory) were used. HUVECs and hPSC-VSMCs at a ratio of 1:1 were added to the Matrigel mixture to a final concentration of 10 million cells/mL. The Matrigel mixture (300 μL) was then immediately engrafted subcutaneously into the dorsal flank of the mouse. Two implants were engrafted per animal. Implants were recovered after 14 days, then the implants were excised. They were fixed in 4% PFA. Immunostaining of human CD31 (HUVECs) and human PDGFRB (hPSC-VSMCs) was performed to analyze the tube formation potential *in vivo*. Three mice for each group were used for the Matrigel plug assay. Mean number of vessel-associated VSMCs per mm vessel length was assessed by ImageJ software.

2.10. RNA sequencing and data analysis

Total RNA of all VSMCs were prepared with RNeasy mini kit (cat # 74104 QIAGEN) according to the manufacturer's instruction. Prior to RNA sequencing, magnetic beads coated with anti-CD144 antibodies were added to remove CD144+ hPSC-ECs with a magnetic cell separator. VSMCs reached 95% purity after purification. Libraries were prepared with TruSeq Stranded mRNA Library Prep Kit and sequenced with Illumina NextSeq 500.20 million 75 bp paired-end reads were generated for each sample. The thresholds for differential expression were set at fold-change >2 and adjusted P-values <0.001 for the null hypothesis. Methods for the data processing, heatmap generating, PCA analysis, differential gene expression analysis have been described in our previous publication [30].

2.11. Statistical analysis

The data are presented as the mean ± standard deviation (SD) from three independent experiments. We used an unpaired t-test to compare two groups and one-way ANOVA to compare more than two groups. A sample size of 3 was selected so that at a significance level of 0.05 there at least 95% chance of detecting two SD's difference in outcome between the groups. All data were processed using GraphPad Prism 8 (GraphPad Software, Inc., La Jolla, CA).

2.12. Accession numbers

The accession numbers for the data reported in this paper are GEO: GSE99776 and GSE109683.

3. Results

3.1. hPSC expansion and differentiation in four culture methods

We first checked and confirmed the quality of H9 hESCs in our previous studies [29,35–38]. Processing and culturing hPSCs in 3D-PNIPAAm-PEG hydrogel [15] and 3D alginate hydrogel fiber [30] are described in our previous publications and Methods (Fig. 1). hPSCs were expanded and differentiated in different culture methods (Fig. 2A and B) and characterized based on our previous report [39]. Live/dead cell staining revealed that initiating hPSCs from different methods were good (Fig. 2C). An efficient and simple protocol of VSMCs differentiation from hPSCs reported by Patsch [20] has been established in 2D monolayer level in 6 days for various biological applications (Fig. 2A). After 5 days differentiation, the typical morphologies of VSMCs derived from 2D and transferring 3D

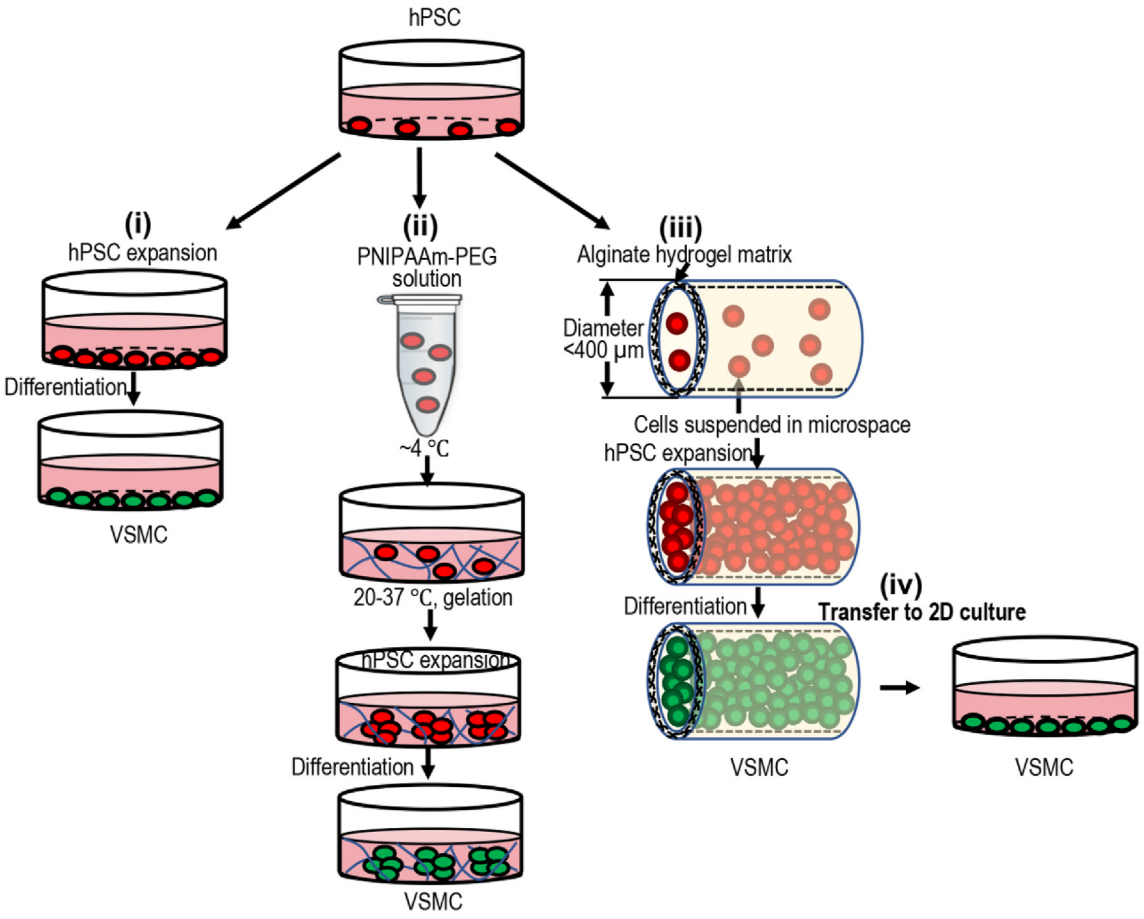

Fig. 1. Overview of different culture methods for hPSCs-VSMC differentiation. (**i**) Two-dimensional (2D) culture system. (**ii**) Three dimensional (3D) PNIPAAm-PEG hydrogel culture system. Single hPSCs are mixed with 10% PNIPAAm-PEG solution at low temperature (e.g., 4 °C), which forms an elastic hydrogel at 37 °C. Single hPSCs clonally expand into uniform spheroids in the hydrogel in 5 days, followed by hPSCs differentiation into VSMCs in the hydrogel. (**iii**) Three-dimensional (3D) alginate hydrogel culture system. hPSC are processed into the alginate hydrogel tubes at low seeding density and expanded for 9 days to fill the tubes. Once the targeted cell number of hPSCs is reached, hPSCs (around day 5) can be differentiated into VSMCs in the alginate hydrogel. (**iv**) Harvested VSMCs from 3D-alginate hydrogel system were transferred to 2D culture for 6 days.

alginate hydrogel culture to 2D culture were observed, and 3D methods also showed good quality of VSMCs by morphologies observation (Fig. 2D). Immunostaining showed majority of VSMCs were SM22A+ and α-SMA+ (Fig. 2E and F). About 24-fold, 2.4×10^7 cells/mL in 3D-PEG hydrogel, and about 410-fold, 4.1×10^8 cells/mL in 3D-Alginate hydrogel was produced on day 10, respectively compared with about 15-fold, 1.5×10^7 cells/mL in 2D culture (Fig. 2G and H).

3.2. Properties of all VSMCs made in four culture methods

To investigate whether the VSMCs produced from four different culture methods displayed similar properties, we performed *in vitro* and *in vivo* functional assay. The fibronectin deposition assay and Western blot analysis showed 3D methods had higher fibronectin production and expression in response to TGF-β (Fig. 3A–C). For the tube formation assays, 2.0×10^4 HUVECs per cm^2 and 2.0×10^4 hPSC-VSMCs per cm^2 were prestained with DiI (red) and DiO (green), respectively, then were co-cultured for 24 h in the incubator. When co-cultured with HUVECs, all groups could form the vascular-like structures, and 3D methods displayed slightly higher mean number of vessels associated VSMCs per 0.5 mm vessel length (Fig. 3D and E). For contractile assay, VSMCs were seeded in N2B27 containing 2 ng/mL Activin-A and 2 μg/mL at 40,000 cells per cm^2 on Collagen-coated wells for 48 h. Then the cells were stained with 2.5 μM Fluo-4 AM at 37 °C for 1 h, followed by 100 μM carbachol treatment. Hydrogel-based groups had better contraction in response to carbachol treatment using ImageJ analysis function (Fig. 3F–H). Calcium imaging by measuring relative fluorescent change of the same cell using ImageJ analysis function revealed that the carbachol-induced a temporary increase in intracellular calcium levels (Fig. 3I). For Matrigel plug assay, the Matrigel mixture (300 μL) containg HUVECs and hPSC-VSMCs was engrafted subcutaneously into the dorsal flank of the immunodeficient mouse for 14 days. The results revealed that hydrogel-based groups showed better vascular like structure in the matrix (Fig. 3J and K).

3.3. Transcriptomic analysis of hPSCs-VSMCs from different methods

To investigate differential expression genes (DGEs), the whole transcriptome analysis by sequencing the mRNAs was performed including the undifferentiated H9s, VSMC_2D, VSMC_3D, VSMC_F, and VSMC_F-d6 (3 biological replicates for each group). Hierarchical clustering heat map showed all produced VSMCs clustered closely and were very different from the undifferentiated H9s (Fig. 4A). Principle components analysis (PCA) showed slightly DGEs among VSMC_2D, VSMC_F and VSMC_F-d6, while VSMC_3D displayed different gene expression at PC2 components compared

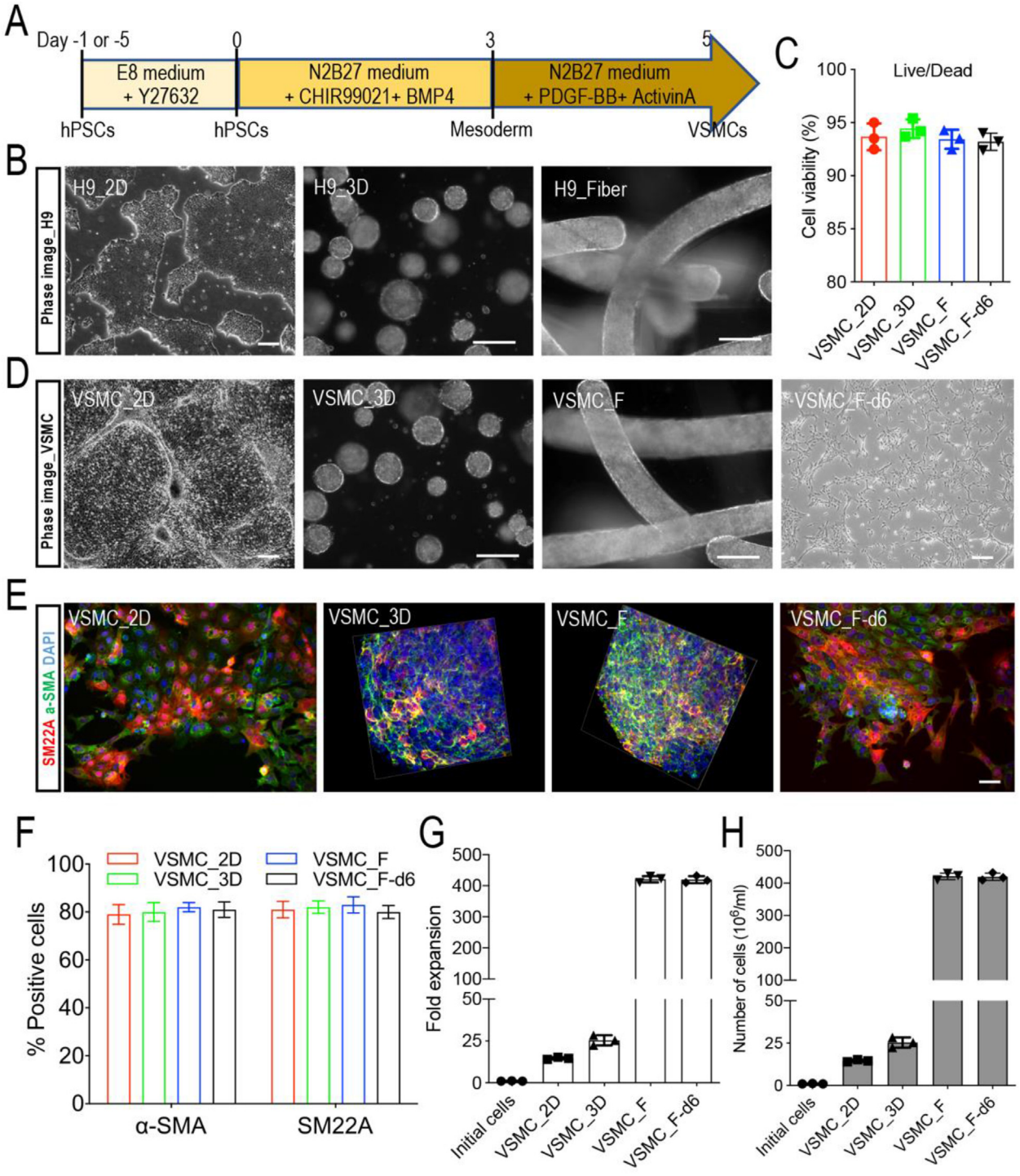

Fig. 2. The comparison of hPSCs derived VSMCs in different culture systems (**A**) Schematic illustration of the VSMC differentiation protocol (**B**) Phase images of hPSC (H9) in different culture systems. Scale bar, 200 μm (**C**) Live/dead staining of harvested cells from 2D, 3D-PEG and 3D-Alginate culture system (n = 3) (**D**) Phase images of hPSC-VSMCs on day 5 in different culture systems. Scale bar, 200 μm (**E**) Immunostaining analysis of VSMC markers SM22A and α-SMA on day 5 cells. Scale bar, 50 μm (**F**) Statistical analysis of differentiation efficiency for VSMC markers SM22A and α-SMA on day 5 cells (n = 3) (**G, H**) When seeded at 1.0×10^6 cells/mL, ~15-, ~24- and ~410-fold expansion, yielding ~1.5×10^7 VSMCs/mL, 2.4×10^7 VSMCs/mL PEG hydrogel and ~4.1×10^8 VSMCs/mL alginate hydrogel are produced in 2D, 3D-PEG and 3D-Alginate culture system, respectively. Data are presented as mean ± SD of three independent replicates (n = 3). **p < 0.01, ****p < 0.0001.

to other VSMCs, but very different from H9s (Fig. 4B). The correlation coefficients between VSMC_3D/VSMC_2D, VSMC_F/VSMC_2D, VSMC_F-d6/VSMC_2D were >0.79, >0.78 and > 0.81 respectively, while among all groups, both VSMC_F and VSMC_F-d6 showed higher correlation coefficients, indicating they were derived from 3D-alginate hydrogel method (Fig. 4C). Gene Ontology (GO) term showed that both VSMC_3D/VSMC_2D and VSMC_F-d6/VSMC_2D are enriched in vasculature development, blood vessel development, cardiovascular system development, angiogenesis, while VSMC_F/VSMC_2D are enriched in

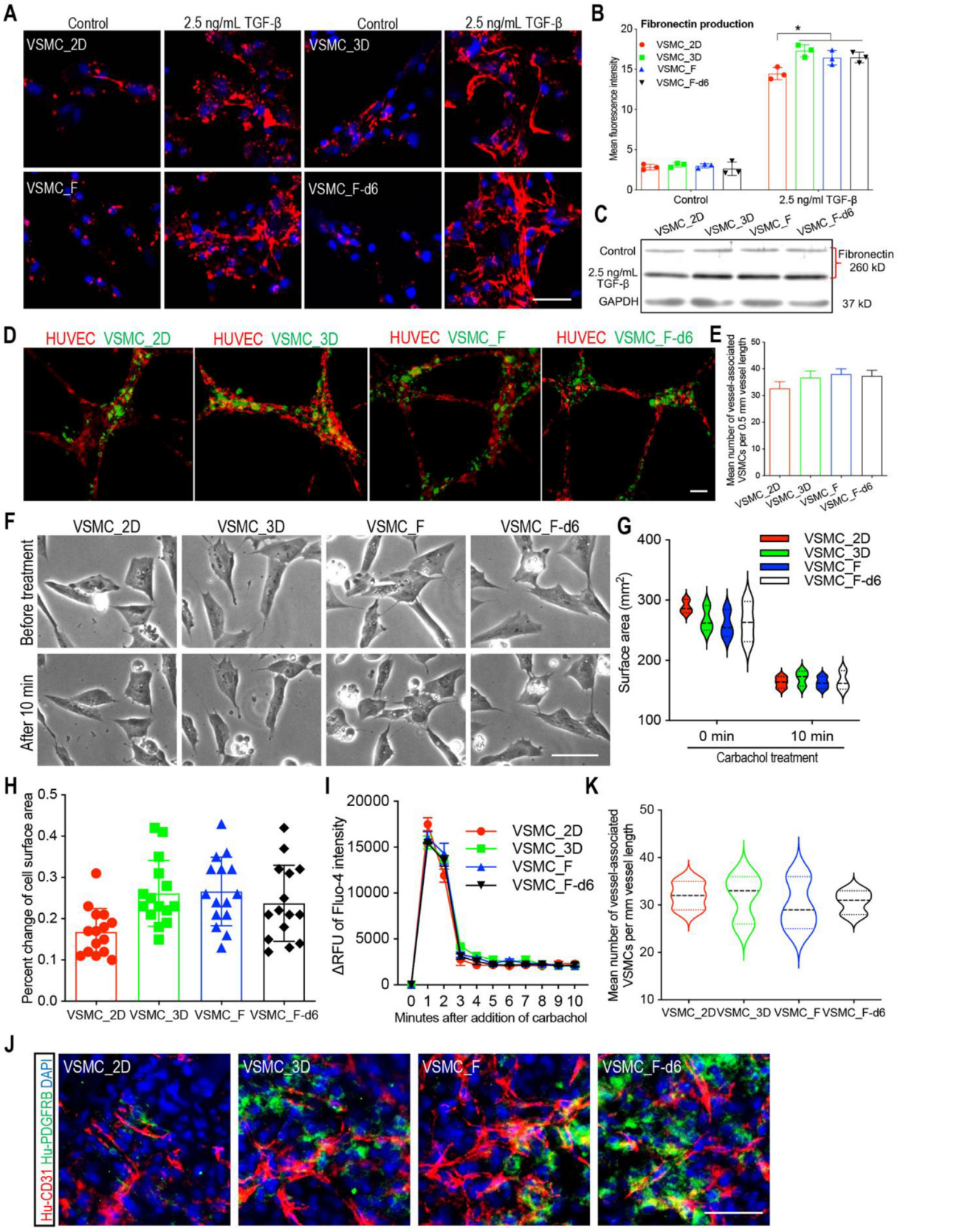

Fig. 3. Properties of hPSC-VSMCs made in different culture systems (A) Immunostaining of fibronectin production of VSMC_2D, VSMC_3D, VSMC_F and VSMC_F-d6 after 24 h of 2.5 ng/mL TGF-β treatment **(B)** Quantification of produced fibronectin. Data are represented as mean ± SD (n = 3). Scale bar, 50 μm **(C)** Western blot analysis of produced fibronectin. GAPDH was as the control **(D, E)** Co-culture of VSMCs and HUVECs and statistical analysis of number of VSMCs attached to the vessels (**E**). Scale bar, 50 μm **(F–H)** Phase images **(F)**, surface area **(G)** and percent change of cell surface area (n = 15) **(H)** of VSMC_2D, VSMC_3D, VSMC_F and VSMC_F-d6 in response to carbachol treatment. Data are represented as mean ± SD. Scale bar, 50 μm **(I)** The relative fluorescence unit (ΔRFU) of Fluo-4 loaded VSMCs over 10 min after adding carbachol. Data are represented as mean ± SD (n = 3) **(J, K).**

extracellular matrix organization, muscle tissue development, muscle organ development, endothelium development (Fig. 4D).

A Venn diagram showed that 157 genes and 3897 genes were significantly upregulated and downregulated in all VSMCs, respectively; and 165 upregulated genes and 665 downregulated genes in VSMC_2D, VSMC_F, and VSMC_F-d6 samples; 123 upregulated genes and 256 downregulated genes in VSMC_3D, VSMC_F, and VSMC_F-d6 samples; 53 upregulated genes and 201 downregulated genes in VSMC_2D, VSMC_3D, and VSMC_F samples; 21 upregulated genes and 258 downregulated genes in VSMC_2D, VSMC_3D, and VSMC_F-d6 samples (Fig. 5A and B), which drove us to perform differential gene expression analysis. Detailed gene expression of the RNA-Seq showed the following differences in VSMC_2D, VSMC_3D, VSMC_F, and VSMC_F-d6 according to regulation of VSMC adhesion, migration, proliferation and cytoskeletal arrangement [40]: (**a**) For collagens gene expression: COL3A1, COL1A2, COL24A1, COL12A1, COL25A1, COL22A1, COL16A1, COL15A1, COL14A1 were higher expression in VSMC_F group compared to other two groups, indicating VSMC_F may have great tensile strength; For laminins gene expression: LAMA1, LAMA4, LAMB4 and LAMA3 were co-downregulated among VSMC_3D, VSMC_F, and VSMC_F-d6, but LAMB3, LAMC2 were only higher expression in VSMC_3D, LAMC3 was only higher expression in VSMC_F-d6, indicating VSMC_3D may hold better adhesive capability (Fig. 5D); For integrins expression [40], ITGA10 and ITGA11 were co-upregulated among VSMC_3D, VSMC_F, and VSMC_F-d6, while ITGA2 was higher expressed in VSMC_3D and VSMC_F, ITGA1 was higher expressed in VSMC_F and VSMC_F-d6, and ITGB3 was only higher expressed in VSMC_3D and downregulated in VSMC_F-d6 (Fig. 5E). For proteases gene expression: MMP9, MMP1, MMP16 were co-upregulated among VSMC_3D, VSMC_F, and VSMC_F-d6; TIMP2, MMP19, TIMP3, MMP11, MMP17 were co-downregulated among VSMC_3D, VSMC_F, and VSMC_F-d6; and other ECM components: DCN, THBS2, VWF, THSD1, NTN1, TNC were co-upregulated among VSMC_3D, VSMC_F, and VSMC_F-d6, but EFEMP1, FBLN5 were higher expression in VSMC_3D and VSMC_F, and FN1 was higher expression in VSMC_F, and VSMC_F-d6 (Fig. 5F and G); (**b**) For glycolysis gene expression, ALDOA, ENO1, ENO2, HK2, PGK1, TPI1 were only higher expression in VSMC_3D; PGAM2 was co-upregulated among VSMC_3D, VSMC_F, and VSMC_F-d6, indicating that VSMC_3D may display higher glycolysis activity (Fig. 5H); (**c**) For angiogenesis associated gene expression, EMCN, IGF1, DLL4, LMO2, NOTCH4, FGF10, SOX18, MMP9, NPR1, SOX17, PTGS2, IL1B, VEGFB were co-upregulated among VSMC_3D, VSMC_F, and VSMC_F-d6; IL6, NOS3, PDGFA, TGFA were co-downregulated among VSMC_3D, VSMC_F, indicating their may have similar angiogenesis capability (Fig. 5I).

3.4. Marker gene expression of VSMC derived from different methods

We also compared the differences of cell cycle, cell apoptosis and cell differentiation at transcriptional levels between VSMC_3D, VSMC_F and VSMC_F-d6. The significantly co-upregulated genes BCL2, CDKN2A, CDKN2B, and the opposite gene expression E2F1, ARUKB, CDC25C which higher expression in VSMC_F to promote cell proliferation were shown in cell cycle (Fig. 6A). The significantly upregulated genes BCL2, BNIP3, TNFRSF10A, and TNF were shown in cell apoptosis in VSMC_F group, but CASP3 as executors of apoptosis was not obviously expressed in cell apoptosis (Fig. 6B). In cell differentiation, BMP2, BMP4, BMP5, FGF1 and OSCIN1 was significantly upregulated in VSMC_F (Fig. 6C). Finally, we confirmed some interesting genes expression by quantitative RT-PCR. We use qRT-PCR to quantitatively analyze several genes including α-SMA, SM22A, Calponin, VEGFA, VEGFB, VEGFC, FN and COL4A. VSMC_2D and VSMC_F-d6 had higher expression of α-SMA, SM22A and Calponin, and VSMC_3D and VSMC_F showed higher expression of Smoothelin (SMTN). VSMC_3D and VSMC_F had higher expression of VEGFA, VEGFC, FN and COL4A6 compared to VSMC_and 2D VSMC_F-d6 (Fig. 6D). These results suggested that 3D conditions held relatively high proliferative capacity and functional phenotype, implicating their suitable for large-scale cell production.

4. Discussion

VSMCs are mainly obtained either in human tissues or *in vitro* culture. However, obtaining large numbers of primary VSMCs from human tissues are very challenging due to the ethical concerns. In addition, *in vitro* 2D culture is not suitable for some specific cell types because of proliferative limitation and phenotypic change, and small scale production due to its time consuming [27]. 3D suspension culturing leads to big cell agglomerates, leading to low cell production, cell death and spontaneous differentiation [27]. Thus, developing novel culture methods for large scale production of hPSCs and derivatives for biomedical applications are needed. In this study, we presented four different culture methods for hPSCs (Fig. 1) and their derivatives based on our previous reports [29,35–38], and systematically evaluated their functional properties and the whole transcriptomic changes. We found hPSC-VSMCs produced from four culture methods had similar contractile phenotypes and the potential of vasculature formation (Fig. 3). The transcriptomic analysis showed the hydrogel-based culture methods displayed more upregulated genes in vasculature development, blood vessel development and angiogenesis, extracellular matrix compared with 2D culture (Fig. 4). Unlike our previous studies, here we systematically compare the all aspects of different culture methods, including cell yield (Fig. 2), differentiation efficiency (Fig. 2), functions (Fig. 3), gene expression (Figs. 4–6), and to determine which is more suitable for industrial production in future.

3D PNIPAAm PEG hydrogel [33] and alginate hydrogel [38] are optimized to expand hPSCs and differentiate hPSCs into VSMCs based on our previous studies [29,35–38]. In this paper, we compared hPSC-VSMCs derived from four different culture methods. Why we used 3D PNIPAAm-PEG hydrogel for comparison with alginate hydrogel fiber in this study due to the fact that they both offer a number of promising features for GMP-compatible, large-scale culture. In particular, they are synthetic and defined, biocompatible, and enable cell harvest or passaging by simply changing temperature or EDTA treatment. They have the potential to translate into clinical application. And, the high culture efficiency of hydrogel-based culture methods are very attractive for large-scale and high-quality of cell production, especially for 3D alginate hydrogel fiber due to different dimension of microfiber and flat hydrogels. The flat hydrogel was greatly thicker than the microfibers, resulting in limited diffusion of oxygen and nutrients toward the thick hydrogels. The limited diffusion might lead to slow expansion of VSMCs. Although, it seems that further 2D culture after 3D differentiation has some beneficial effects, the process of this method is relatively complicated and expression of VSMC marker genes were not higher than 3D alginate hydrogel fiber. In addition, this method is not suitable for large-scale production in

When VSMCs and HUVECs were co-transplanted subcutaneously, VSMC_2D, VSMC_3D, VSMC_F and VSMC_F-d6 formed nice vascular structures (**J**) with similar number of VSMCs attached to the vessels (**K**). Scale bar, 50 μm. Data are presented as mean ± SD of three independent replicates (n = 3). *p < 0.05.

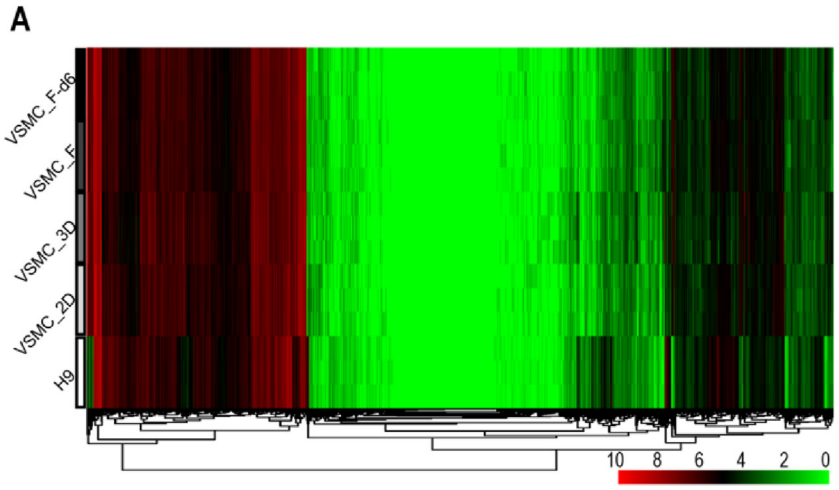

C

	VSMC_2D	VSMC_2D	VSMC_2D	VSMC_3D	VSMC_3D	VSMC_3D	VSMC_F	VSMC_F	VSMC_F	VSMC_F-d6	VSMC_F-d6	VSMC_F-d6
VSMC_2D	1	0.9995	0.9989	0.7943	0.7977	0.8189	0.7804	0.7970	0.7982	0.8194	0.8179	0.8195
VSMC_2D	0.9995	1	0.9991	0.7946	0.7979	0.8194	0.7823	0.7984	0.7997	0.8217	0.8203	0.8219
VSMC_2D	0.9989	0.9991	1	0.7919	0.7955	0.8175	0.7867	0.8010	0.8025	0.8305	0.8292	0.8311
VSMC_3D	0.7943	0.7946	0.7919	1	0.9992	0.9907	0.7482	0.7572	0.7562	0.7497	0.7476	0.7445
VSMC_3D	0.7977	0.7979	0.7955	0.9992	1	0.9915	0.7523	0.7612	0.7602	0.7545	0.7524	0.7495
VSMC_3D	0.8189	0.8194	0.8175	0.9907	0.9915	1	0.8255	0.8339	0.8329	0.7996	0.7974	0.7900
VSMC_F	0.7804	0.7823	0.7867	0.7482	0.7523	0.8255	1	0.9954	0.9962	0.8961	0.8953	0.8737
VSMC_F	0.7970	0.7984	0.8010	0.7572	0.7612	0.8339	0.9954	1	0.9996	0.8738	0.8725	0.8497
VSMC_F	0.7982	0.7997	0.8025	0.7562	0.7602	0.8329	0.9962	0.9996	1	0.8765	0.8753	0.8527
VSMC_F-d6	0.8194	0.8217	0.8305	0.7497	0.7545	0.7996	0.8961	0.8738	0.8765	1	0.9997	0.9981
VSMC_F-d6	0.8179	0.8203	0.8292	0.7476	0.7524	0.7974	0.8953	0.8725	0.8753	0.9997	1	0.9983
VSMC_F-d6	0.8195	0.8219	0.8311	0.7445	0.7495	0.7900	0.8737	0.8497	0.8527	0.9981	0.9983	1

2D: Two dimensional culture; 3D: Three dimensional culture; F: Alginate hydrogel fiber culture; F-d6: Transfer alginate hydrogel fiber culture to 2D culture for 6 days.

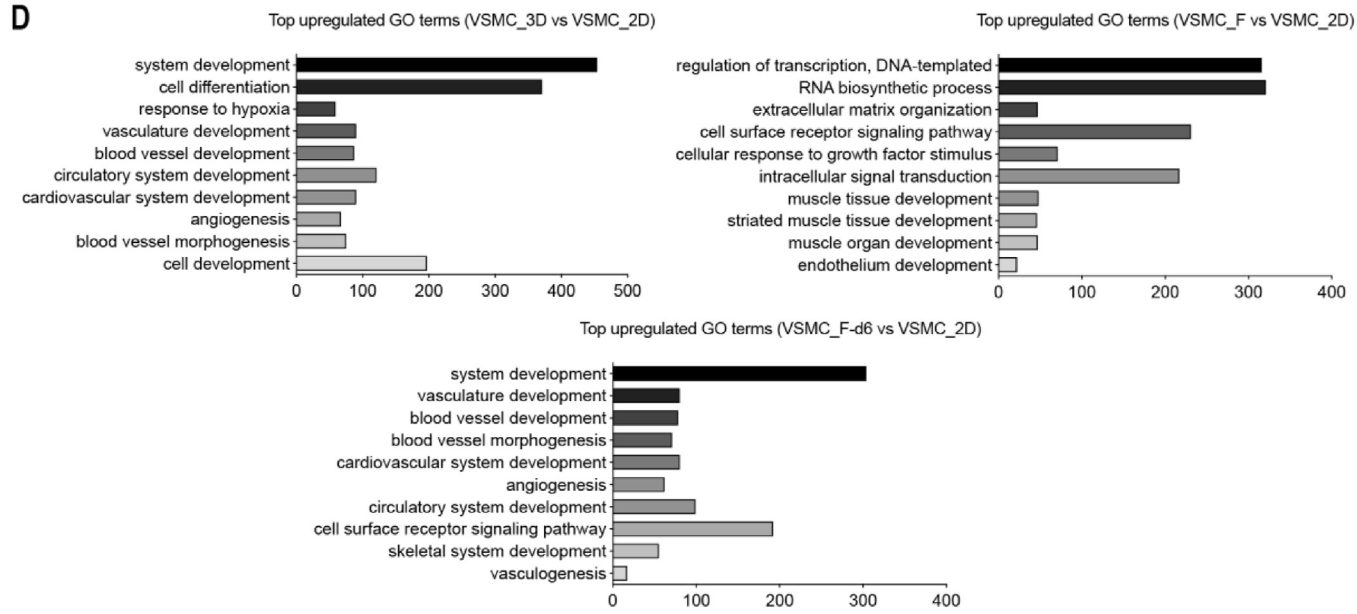

Fig. 4. Whole transcriptome analysis VSMC_F, VSMC_F-d6, VSMC_3D, VSMC_2D derived from H9s (A, B) Global heat map of expressed genes and Principal Component Analysis (PCA) of all VSMCs. Three biological replicates are used for each sample (n = 3) **(C)** The global gene expression correlation coefficients of all VSMC_F, VSMC_F-d6, VSMC_3D, VSMC_2D **(D)** Top 10 upregulated GO terms in VSMC_3D, VSMC_F and VSMC_F-d6 group compared with VSMC_2D, respectively.

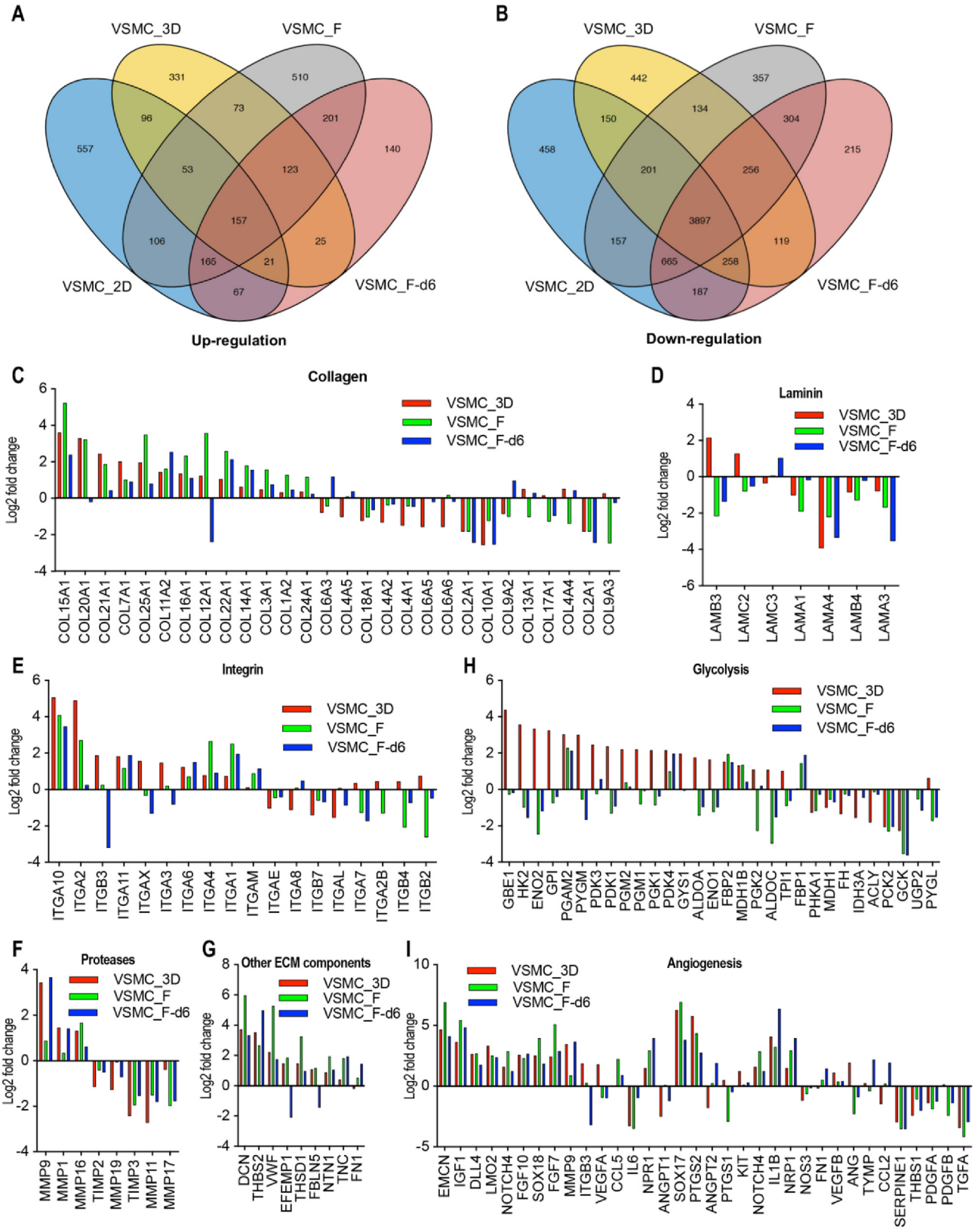

Fig. 5. Differential gene expression analysis among all VSMCs derived from H9s (A, B) Venn diagram showing the up-regulated and down-regulated gene counts in VSMC_2D, VSMC_3D, VSMC_F and VSMC_F-d6 groups **(C–G)** Log 2 (expression level in VSMC_3D, VSMC_F and VSMC_F-d6/expression level in VSMC_2D) of extracellular matrix genes **(H, I)** Log2 (expression level in VSMC_3D, VSMC_F and VSMC_F-d6/expression level in VSMC_2D) of genes related to glycolysis **(H)**, and angiogenesis **(I).** In Fig. 5C–I, VSMC_2D was as a control group.

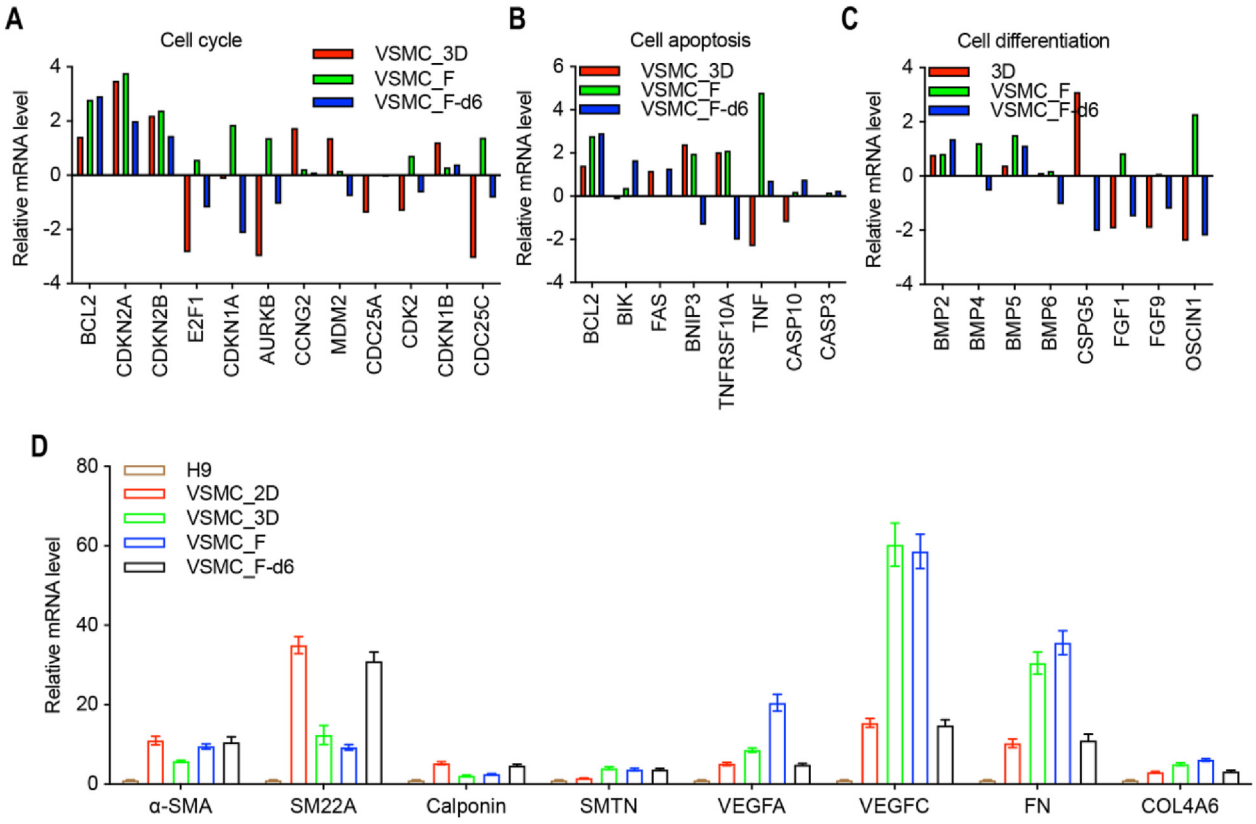

Fig. 6. Differential gene expression analysis between hydrogel-based VSMCs derived from H9s (A–C) Log 2 (expression level in VSMC_3D, VSMC_F and VSMC_F-d6/expression level in VSMC_2D) of cell cycle (A), cell apoptosis(B) and cell differentiation (C). VSMC_2D was as a control group (D) qRT-PCR analyses of VSMC_2D, VSMC_3D, VSMC_F and VSMC_F-d6 for synthetic VSMC markers α-SMA, SM22A and Calponin, and contractile VSMC marker SMTN, and other genes related to VSMCs including growth factors VEGFA and VEGFC, and ECM genes FN and COL4A. Data are represented as mean ± SD of three biological replicates (n = 3). *p < 0.05, **p < 0.01, ***p < 0.001, ****p < 0.0001.

industrial production. High quality cells have irreplaceable advantages in cell therapy, tissue engineering. The hydrogel-based culture methods eliminate large agglomeration and shear force. hPSC derived VSMCs produced in alginate hydrogel fiber (~4.1 × 10^8 cells/mL) is about 200 times of cell yield in 3D suspension culturing and ~20 times in 3D-PEG hydrogel culture system [15,30]. In addition, alginates are non-toxic and clinical-grade materials, affordable and available [41]; mechanically and chemically stable, transparent, and alginate fibers provide very friendly microenvironment to prevents cells agglomeration. In addition, previous studies reported that high cell density affected the stemness genes expression [42] and cell behavior [43] due to over aggregation of cells resulting in apoptosis/necrosis and uncontrolled differentiation in the core of cell aggregates. In our study, we demonstrated that 3D culture methods, especially for 3D alginate hydrogel, limited the over aggregation by controlling the size, which not only efficiently transport the nutrients and oxygen, but also lead to high culture efficiency. It is the innovation of cell culture technology. Therefore, this study provided the direct evidence for alginate hydrogel fiber used in industrial production.

5. Conclusion

In summary, we systematically compared hPSC-VSMCs generated from four different culture methods, and demonstrated that alginate hydrogel-based culture method will become a versatile culture system for hPSCs and their derivatives in various biological applications and industrial production.

Author contributions

Conceptualization, Yuguo Lei, Zhanqi Wang and Haishuang Lin; Data curation, Qing Liu, Hongyu Gu and Xuesheng Wu; Formal analysis, Hongyu Gu, Yuxia Ge, and Xuesheng Wu; Funding acquisition, Zhanqi Wang, Qing Liu and Fuxing Zuo; Methodology, Yuxia Ge and Zhen Liu; Project administration, Qing Liu and Hongyu Gu; Software, Qian Du; Writing – original draft, Zhanqi Wang and Haishuang Lin; Writing – review & editing, Haishuang Lin, Zhen Liu and Fuxing Zuo. All authors have read and agreed to the published version of the manuscript.

Data availability

The authors declare that all data supporting the results in this study are available within the paper.

Declaration of competing interest

The authors declare no competing financial interest.

Acknowledgements

This work was supported by the National Natural Science Foundation of China (Grant No. 82000449), Basic-Clinical Research Cooperation Fund of Capital Medical University (No. 16JL90) and CAMS Innovation Fund for Medical Science (CIFMS) (2020-I2M-C&T-B-071).

References

[1] Owens GK, Kumar MS, Wamhoff BR. Molecular regulation of vascular smooth muscle cell differentiation in development and disease. Physiol Rev 2004;84:767–801.

[2] Carmeliet P. Mechanisms of angiogenesis and arteriogenesis. Nat Med 2000;6:389–95.

[3] Biel NM, Santostefano KE, DiVita BB, DiVita BB, Rouby NE, Carrasquilla SD, et al. Vascular smooth muscle cells from hypertensive patient-derived induced pluripotent stem cells to advance hypertension pharmacogenomics. Stem Cells Transl Med 2015;4:1380–90.

[4] Ji H, Kim HS, Kim H-W, Leong KW. Application of induced pluripotent stem cells to model smooth muscle cell function in vascular diseases. Curr Opin Biomed Eng 2017;1:38–44.

[5] Ge X, Ren Y, Bartulos O, Lee MY, Yue Z, Kim KY, et al. Modeling supravalvular aortic stenosis syndrome with human induced pluripotent stem cells. Circulation 2012;126:1695–704.

[6] Granata A, Serrano F, Bernard WG, McNamara M, Low L, Sastry P, et al. An iPSC-derived vascular model of Marfan syndrome identifies key mediators of smooth muscle cell death. Nat Genet 2017;49:97–109.

[7] Levenberg S. Engineering blood vessels from stem cells: recent advances and applications. Curr Opin Biotechnol 2005;16:516–23.

[8] Wang Y, Hu J, Jiao J, Liu Z, Zhou Z, Zhao C, et al. Engineering vascular tissue with functional smooth muscle cells derived from human iPS cells and nanofibrous scaffolds. Biomaterials [Internet] 2014;35:8960–9. Available at: https://doi.org/10.1016/j.biomaterials.2014.07.011.

[9] Karamariti E, Margariti A, Winkler B, Wang X, Hong X, Baban D, et al. Smooth muscle cells differentiated from reprogrammed embryonic lung fibroblasts through dkk 3 signaling are potent for tissue engineering of vascular grafts. Circ Res 2013;112:1433–43.

[10] Ye L, Chang YH, Xiong Q, Zhang P, Zhang L, Somasundaram P, et al. Cardiac repair in a porcine model of acute myocardial infarction with human induced pluripotent stem cell-derived cardiovascular cells. Cell Stem Cell 2014;15:750–61.

[11] Hong X, Margariti A, Bras AL, Jacquet L, Wei Kong W, Hu Y, et al. Trans-differentiated human vascular smooth muscle cells are a new potential cell source for endothelial regeneration. Sci Rep 2017;7:5590.

[12] Cheung C, Bernardo AS, Pedersen RA, Sinha S. Directed differentiation of embryonic origin-specific vascular smooth muscle subtypes from human pluripotent stem cells. Nat Protoc 2014;9:929–38.

[13] Poh M, Boyer M, Solan A, Dahl S, Pedrotty D, Banik S, et al. Blood vessels engineered from human cells. Lancet 2005;365:2122–4.

[14] Chen G, Gulbranson D, Hou Z, Bolin J, Ruotti V, Probasco M, et al. Chemically defined conditions for human iPSC derivation and culture. Nat Methods 2011;8:424–9.

[15] Lei Y, Schaffer DV. A fully defined and scalable 3D culture system for human pluripotent stem cell expansion and differentiation. Proc Natl Acad Sci U S A 2013;110:E5039–48.

[16] Okita K, Matsumura Y, Sato Y, Okada A, Morizane A, Okamoto S, et al. A more efficient method to generate integration-free human iPS cells. Nat Methods 2011;8:409–12.

[17] Takahashi K, Tanabe K, Ohnuki M, Narita M, Ichisaka T, Tomoda K, et al. Induction of pluripotent stem cells from adult human fibroblasts by defined factors. Cell 2007;131:861–72.

[18] Lin B, Kim J, Li Y, Pan H, Vergara XC, Salama G, et al. High-purity enrichment of functional cardiovascular cells from human iPS cells. Cardiovasc Res 2012;95:327–35.

[19] Lee TH, Song SH, Kim KL, Yi JY, Shin GH, Kim JY, et al. Functional recapitulation of smooth muscle cells via induced pluripotent stem cells from human aortic smooth muscle cells. Circ Res [Internet] 2010;106:120–8. Available at: http://circres.ahajournals.org/cgi/doi/10.1161/CIRCRESAHA.109.207902.

[20] Patsch C, Challet-Meylan L, Thoma E, Urich E, Heckel T, Sullivan J, et al. Generation of vascular endothelial and smooth muscle cells from human pluripotent stem cells. Nat Cell Biol 2015;17:994–1003.

[21] Cheung C, Bernardo AS, Trotter MWB, Pedersen RA, Sinha S. Generation of human vascular smooth muscle subtypes provides insight into embryological origin–dependent disease susceptibility. Nat Biotechnol 2012;30:165–73.

[22] Bernardo A, Faial T, Gardner L, Niakan K, Ortmann D, Senner C, et al. BRACHYURY and CDX2 mediate BMP-induced differentiation of human and mouse pluripotent stem cells into embryonic and extraembryonic lineages. Cell Stem Cell [Internet] 2011;9:144–55. Available at: https://doi.org/10.1016/j.stem.2011.06.015.

[23] Wanjare M, Kuo F, Gerecht S. Derivation and maturation of synthetic and contractile vascular smooth muscle cells from human pluripotent stem cells. Cardiovasc Res 2013;97:321–30.

[24] Wanjare M, Agarwal N, Gerecht S. Biomechanical strain induces elastin and collagen production in human pluripotent stem cell-derived vascular smooth muscle cells. Am J Physiol Cell Physiol 2015;309:C271–81.

[25] Bajpai VK, Mistriotis P, Loh Y-H, Daley GQ, Andreadis ST. Functional vascular smooth muscle cells derived from human induced pluripotent stem cells via mesenchymal stem cell intermediates. Cardiovasc Res [Internet] 2012;96:391–400. Available at: https://academic.oup.com/cardiovascres/article-lookup/doi/10.1093/cvr/cvs253.

[26] Eoh J, Shen N, Burke J, Hinderer S, Xia Z, Schenke-Layland K, et al. Enhanced elastin synthesis and maturation in human vascular smooth muscle tissue derived from induced-pluripotent stem cells. Acta Biomater [Internet] 2017;52:49–59. Available at: https://doi.org/10.1016/j.actbio.2017.01.083.

[27] Kropp C, Massai D, Zweigerdt R. Progress and challenges in large-scale expansion of human pluripotent stem cells. Process Biochem 2017;59:244–54.

[28] Jenkins MJ, Farid SS. Human pluripotent stem cell-derived products : advances towards robust , scalable and cost-effective manufacturing strategies. Biotechnol J 2015;10:83–95.

[29] Lin H, Du Q, Li Q, Wang O, Wang Z, Liu K, et al. A hydrogel-based bioprocess for scalable manufacturing of human pluripotent stem cells-derived neural stem cells. ACS Appl Mater Interfaces [Internet] 2018;10:29238–50. Available at: http://pubs.acs.org/doi/10.1021/acsami.8b05780.

[30] Li Q, Lin H, Du Q, Liu K, Wang O, Evans C, et al. Scalable and physiologically relevant microenvironments for human pluripotent stem cell expansion and differentiation. Biofabrication 2018;10:025006.

[31] Lin H, Li Q, Wang O, et al. Automated expansion of primary human T cells in scalable and cell-friendly hydrogel microtubes for adoptive immunotherapy. Adv Healthc Mater 2018;7:e1701297.

[32] Li Q, Lin H, Rauch J, Deleyrolle L, Reynolds B, Viljoen H, et al. Scalable culturing of primary human glioblastoma tumor-initiating cells with a cell-friendly culture system. Sci Rep 2018;8:3531.

[33] Lin H, Du Q, Li Q, Wang O, Wang Z, Neety Sahu N, et al. A scalable and efficient bioprocess for manufacturing human pluripotent stem cells-derived endothelial cells. Stem Cell Rep 2018;11:454–69.

[34] Matsumoto H, Moir L, Oliver B, Burgess J, Roth M, Black J, et al. Comparison of gel contraction mediated by airway smooth muscle cells from patients with and without asthma. Thorax [Internet] 2007;62:848–54. Available at: http://thorax.bmj.com/cgi/doi/10.1136/thx.2006.070474.

[35] Lin H, Li Q, Lei Y. An integrated miniature bioprocessing for personalized human induced pluripotent stem cell expansion and differentiation into neural stem cells. Sci Rep [Internet] 2017;7:40191. Available at: http://www.nature.com/articles/srep40191.

[36] Lin H, Qiu X, Du Q, Li Q, Wang O, Akert L, et al. Engineered microenvironment for manufacturing human pluripotent stem cell-derived vascular smooth muscle cells. Stem Cell Rep [Internet] 2019;12:84–97. Available at: https://doi.org/10.1016/j.stemcr.2018.11.009.

[37] Lin H, Li Q, Du Q, Wang O, Wang Z, Akert L, et al. Integrated generation of induced pluripotent stem cells in a low-cost device. Biomaterials [Internet] 2019;189:23–36. Available at: https://doi.org/10.1016/j.biomaterials.2018.10.027.

[38] Lin H, Du Q, Li Q, Wang O, Wang Z, Elowsky C, et al. Manufacturing human pluripotent stem cell derived endothelial cells in scalable and cell-friendly microenvironments. Biomater Sci 2019;7:373–88.

[39] Wang Z, Zuo F, Liu Q, Wu X, Du Q, Lei Y, et al. Comparative study of human pluripotent stem cell-derived endothelial cells in hydrogel-based culture systems. ACS Omega 2021;6:6942–52.

[40] Brooke BS, Karnik SK, Li DY. Extracellular matrix in vascular morphogenesis and disease: structure versus signal. Trends Cell Biol 2003;13:51–6.

[41] Yong K, Mooney DJ. Alginate: properties and biomedical applications. Prog Polym Sci 2012;37:106–26.

[42] Kim D, Lee M, Lee TH, Sung K, Koo H, Yoo K. Cell culture density affects the stemness gene expression of adipose tissue-derived mesenchymal stem cells. Biomed Reports 2017;6:300–6.

[43] Kim MH, Thanuthanakhun N, Fujimoto S, Kino-oka M. Effect of initial seeding density on cell behavior-driven epigenetic memory and preferential lineage differentiation of human iPSCs. Stem Cell Res [Internet 2021;56:102534. Available at: https://doi.org/10.1016/j.scr.2021.102534.